



NIH Public Access

Author Manuscript

J Am Chem Soc. Author manuscript; available in PMC 2012 March 23.

Published in final edited form as:

J Am Chem Soc. 2011 March 23; 133(11): 3863–3868. doi:10.1021/ja107033v.

Single-step Charge Transport through DNA over Long Distances

Joseph C. Genereux, Stephanie M. Wuerth, and Jacqueline K. Barton*

Division of Chemistry and Chemical Engineering, California Institute of Technology, Pasadena, California 91125, USA

Abstract

Quantum yields for charge transport across adenine tracts of increasing length have been measured by monitoring hole transport in synthetic oligonucleotides between photoexcited 2-aminopurine, a fluorescent analogue of adenine, and N₂-cyclopropyl guanine. Using fluorescence quenching, a measure of hole injection, and hole trapping by the cyclopropyl guanine derivative, we separate the individual contributions of single- and multi-step channels to DNA charge transport, and find that with 7 or 8 intervening adenines the charge transport is a coherent, single-step process. Moreover, a transition occurs from multi-step to single-step charge transport with increasing donor/acceptor separation, opposite to that generally observed in molecular wires. These results establish that coherent transport through DNA occurs preferentially across 10 base pairs, favored by delocalization over a full turn of the helix.

INTRODUCTION

The exceptional ability of DNA to mediate charge transport (CT) is the basis of novel molecular devices and may be exploited by the cell for both redox sensing and signaling.¹ The conduction properties of different DNA assemblies are found to be highly sensitive not only as to how the DNA is coupled within a particular assay but also as to how the DNA base pairs are dynamically stacked.² As a consequence, the sequence-dependent yields of DNA-mediated CT are not readily rationalized with superexchange and hopping through static structures.^{2,3}

DNA CT is mediated by the π -stack of the base pairs, and for well-coupled donors and acceptors, can lead to charge migration over 200 Å.^{2–4} For the quenching of photoexcited 2-aminopurine (Ap) by guanine across an adenine tract, the distance dependence is shallow but periodic with respect to tract length; the periodicity has been assigned as a consequence of transient delocalization over 4 A-T base pairs being ideal for forming a CT-active state.⁵ Evidence for delocalization has been found from other experimental and theoretical studies.^{6–13} Furthermore, these CT-active states are non-equilibrium states, and their formation is conformationally gated.^{13–16}

DNA CT can also be observed by measuring the chemical decomposition yields of the bases themselves, with guanine being the most reactive to oxidative damage.¹⁷ Guanine degradation after oxidation is measured by strand cleavage at damage sites, or by direct measurement of decomposition products. Because guanine radical decomposition is slow (ms) in the absence of additional reactive species, such as superoxide,¹⁸ this measure of hole arrival is convoluted with the trapping and back electron transfer rates.^{19,20} We have

*To whom correspondence should be addressed. jkbarton@caltech.edu.

Supporting Information Available: Figures S1–S3 and Tables S1 and S2, including complete sequences and CPG decomposition quantum yields. This material is available free of charge via the Internet at <http://pubs.acs.org>.

recently studied CT yield using fast *N*-cyclopropyl radical traps²¹ as substituents on guanine (^{CPG}),^{16,20} adenine (^{C_PA}),²² and cytosine (^{CP}C)⁸ through the exocyclic amines. The subnanosecond decomposition of these traps upon oxidation or reduction allows measurement of pre-equilibrium hole occupation.²⁰ Notably, oxidation of ^{CPG} by a tethered, photoexcited rhodium intercalator has the same periodicity with respect to adenine tract length as does the CT quenching of photoexcited Ap by guanine.¹⁶ Although the ring-opening rates have not been directly measured, there is ample evidence supporting picosecond ring opening, including competition²⁰ with the subpicosecond recombination²³ between ^{CPG} radical cation and thionine radical anion, and competition²⁴ with picosecond recombination²⁵ ($>5 \times 10^{-9} \text{ s}^{-1}$) between ^{CPG} radical cation and aminopurine radical anion. It is also noteworthy that fluorescence spectra for duplexes containing ApA^{CPG} vs. those containing ApAG are identical.²⁴

Here we measure the quantum yields of total CT in comparable assemblies containing Ap and ^{CPG} separated by adenine tracts. Single-step CT yield is obtained from previous measurements of steady-state fluorescence quenching in the same sequences.⁵ In these fluorescence experiments, the differences in Ap emission between sequences with inosine, where there is no CT, and sequences with guanine are compared; the amount of relative quenching from photoexcited Ap reports on the single-step CT to the distant base. This depopulation, detected from the donor, but reliant on the nature of the acceptor, even several base positions away, can only be due to single-step CT between the donor and the acceptor. In multi-step charge transfer to guanine, the initial depopulation of excited aminopurine occurs by oxidation of the bridge. Since substitution of inosine for guanine should not affect this initial step, the inosine-containing duplexes serve as a control for this Ap^{*} relaxation mechanism.

By comparing single step and total charge transport yields, we delineate single-step and multi-step contributions to DNA-mediated charge transport for a series of guanine-terminated adenine tracts (Figure 1). We establish that for some long DNA assemblies, DNA CT is a single step process. These results underscore the importance of long-range, coherent steps in DNA-mediated charge transport across delocalized domains,⁵ and the inadequacy of hopping between localized sites as the sole mechanism for long-range CT through DNA.⁴

EXPERIMENTAL

Oligonucleotide Synthesis

DNA oligonucleotides were synthesized trityl-on using standard phosphoramidite chemistry on an ABI DNA synthesizer with Glen Research reagents. 2-aminopurine (Ap) was incorporated as the *N*₂-dimethylaminomethylidene protected phosphoramidite (Glen Research). ^{CPG}-modified oligonucleotides were prepared by incorporating the precursor base, 2-fluoro-O₆-paraphenylethyl-2'-deoxyinosine (Glen Research), as a phosphoramidite at the desired position.¹⁵ The resin was then reacted with 1 M diaza(1,3)bicyclo[5.4.0]undecane (DBU, Aldrich) in acetonitrile to effectively remove the O₆ protecting group. Similarly, ^{C_PA}-modified oligonucleotides were prepared by incorporating the precursor base, O₆-phenyl-2'-deoxyinosine (Glen Research) as a phosphoramidite at the desired position.²² For both ^{CPG}- and ^{C_PA}-containing strands, the oligonucleotides were subsequently incubated overnight in 6 M aqueous cyclopropylamine (Aldrich) at 60 °C resulting in substitution, base deprotection, and simultaneous cleavage from the resin. The cleaved strands were dried *in vacuo* and purified by reversed-phase HPLC, detritylated by 80% acetic acid for 15 min, and repurified by reversed-phase HPLC. Oligonucleotides were characterized by MALDI-TOF mass spectrometry. Sequences are provided in Table S1.

All oligonucleotides were suspended in a buffer containing 50 mM NaCl, 5 mM sodium phosphate, pH 7 and quantified using UV-visible spectroscopy. Duplexes were prepared by heating equal concentrations of complementary strands to 90 °C for 5 min and slow cooling to ambient temperature.

Photooxidation Experiments

Samples were irradiated at ambient temperature. Duplexes (30 μ L, 10 μ M) in PBS were irradiated on a 1000 W Hg/Xe lamp equipped with a monochromator at 325 nm for 30 sec unless otherwise indicated. To analyze for ^{CP}A or ^{CP}G decomposition following irradiation, samples were digested to the component nucleosides by phosphodiesterase I (USB) and alkaline phosphatase (Roche) to completion. The resulting deoxynucleosides were analyzed by reversed-phase HPLC using a Chemcobond 5-ODS-H, 4.6 mm \times 100 mm column. The amount of ^{CP}G or ^{CP}A per duplex was determined by taking the ratio of the area of the HPLC peak for d ^{CP}G or d ^{CP}A to the area of the peak for dT, the internal reference. The decomposition yield is taken as the percent loss of ^{CP}G or ^{CP}A between an irradiated sample and the dark control; at least nine samples and three dark controls are performed for each sequence. Dark control HPLC traces were quantified for the relative amounts of dA, dC, dG, dI, dT, d ^{CP}A and d ^{CP}G based on duplex sequence, to confirm strand stoichiometry. Actinometry was performed using a 6 mM ferrioxalate standard.²⁶ The given quantum yield is for the efficiency of formation of the ring-opened product per photon absorbed by 2-aminopurine. Errors are presented at 90% standard error of the mean (s.e.m.), using the Student's t-distribution at the appropriate degrees of freedom to determine confidence intervals, and each point represents at least nine replicates.

RESULTS AND DISCUSSION

Duplex Assemblies

To determine the total quantum yield of guanine oxidation by photoexcited Ap, we constructed a series of duplex assemblies with Ap separated from ^{CP}G by adenine tracts of varying length and measured the decomposition of the radical trap upon irradiation. By comparing the yields of total and single-step CT, we determine the relative contributions of single- and multi-step channels (Figure 1). Because ^{CP}G is a fast radical trap, its decomposition yield represents the total yield of all pathways that lead to oxidation of guanine, as long as back electron transfer is slower than ring opening. For direct comparison of guanine and adenine oxidation, we also constructed assemblies containing the ^{CP}A radical trap at various positions along the bridge. We use Ap-A_n- ^{CP}A -A_m-Y to indicate a sequence with an adenine tract of length $n+m+1$, with ^{CP}A at the $n+1$ position, and terminal base Y at the end of the tract (Y = G, I, or ^{CP}G). All eight nucleosides are well resolved by HPLC, allowing straightforward quantification of the ^{CP}G or ^{CP}A content per duplex, and the inosine barriers isolate charge transfer from occurring between the ApA_nY containing region and the rest of the construct.^{15,27}

Quantum Yields for CT

The routes for fluorescence quenching of photoexcited Ap in oligonucleotides have been characterized in detail. The fluorescence of photoexcited Ap in DNA is quenched versus the free nucleoside, even if there is no guanine in the assembly. The presence of a nearby guanine leads to additional quenching of fluorescence by a CT mechanism.^{3,5,24,25,27–29} Adenine oxidation by photoexcited Ap, while favorable, is far slower than guanine oxidation, as is reduction of cytosine and thymidine by photoexcited Ap.²⁵ Recent time-resolved fluorescence and transient absorption measurements have revealed that there is a short-lived (≤ 200 fs) excited state of aminopurine that primarily decays through a dark

state, with a fraction undergoing relaxation to the longer-lived emissive state capable of CT.
30

Based on the known photophysics of aminopurine in DNA, a limit can be inferred for the quantum yield of single-step CT based on the quantum yields of emission from a duplex with a CT-accessible guanine and the analogous duplex replacing guanine with the redox-inactive nucleotide inosine. The relaxation pathways available to an inosine-containing assembly are described in Panel A in Figure S1. It is apparent that

$$\Phi_{em}^I = (1 - \Phi_{nrd})\Phi_{rel \rightarrow em}^I = (1 - \Phi_{nrd}) \frac{k_{em}}{k_{em} + k_A}$$

where Φ_{em}^I is the quantum yield of emission from an inosine-containing duplex, Φ_{nrd} is the quantum yield of hot deactivation through a dark state³⁰, $\Phi_{rel \rightarrow em}$ is the efficiency of emission from the emissive state of aminopurine, k_{em} is the rate of emission from this state, and k_A is the rate of charge transfer to adenine from the emissive state of aminopurine.

For a guanine-containing assembly,

$$\Phi_{em}^G = (1 - \Phi_{nrd})\Phi_{rel \rightarrow em}^G = (1 - \Phi_{nrd}) \frac{k_{em}}{k_{em} + k_A + k_G}$$

where k_G is the rate of charge transfer from the emissive state of aminopurine to guanine across the adenine tract. The quantum yield of CT to guanine is

$$\Phi_{CT}^G = (1 - \Phi_{nrd}) \frac{k_G}{k_{em} + k_A + k_G} = (1 - \Phi_{nrd}) \left(1 - \frac{\Phi_{em}^G}{\Phi_{em}^I} \right)$$

A lower limit can be set on Φ_{CT}^G since

$$\Phi_{em}^I \leq (1 - \Phi_{nrd})$$

and hence

$$\Phi_{CT}^G = (1 - \Phi_{nrd}) \left(1 - \frac{\Phi_{em}^G}{\Phi_{em}^I} \right) \geq \Phi_{em}^I - \Phi_{em}^G$$

This result is intuitive, as the difference between the quantum yields of emission in the presence and absence of guanine is due to single-step CT from aminopurine to guanine.

We therefore compare in Figure 2 the values obtained as lower limits for single step CT measured by fluorescence quenching (red) to our measurements for total CT yield from ^{CPG} decomposition (blue). Upon irradiation, decomposition is observed for ^{CPG}, indicating oxidation of guanine by photoexcited Ap (Table S2). For short donor-acceptor separation ($n = 0-2$), little ring opening occurs, because charge recombination between the aminopurine anion radical and guanine cation radical is competitive with radical trapping at the ^{CPG} (Figure 2).^{16,24} However, with four intervening adenines, ^{CPG} radical decomposition outcompetes charge recombination. The quantum yield for ring opening with respect to generation of excited Ap peaks at about 1% with 4 intervening adenines followed by a slow

decay with longer sequences. The profile for CPG decomposition as a function of distance is similar to that which has previously been observed in other assemblies for oxidation of CPG by photoexcited Ap.16 Interestingly, the peak value is comparable to the quantum yield (1.7%) of emission from Ap-(A)_n-I sequences,⁵ which reflects the maximum yield of CT that can be achieved.

For longer A-tracts, with 4–6 intervening adenines, where charge recombination is not competitive, we see that the quantum yield for single step CT, obtained through fluorescence quenching, does not account for the total CT quantum yield, obtained through CPG decomposition (Figure 2). Photoexcited Ap is competent to oxidize adenine directly, generating a hole that can rapidly migrate across the adenine tract to guanine,^{4,31} and thus some component of multi-step CT is to be expected. Unexpectedly, however, with 7 or 8 intervening adenines, the quantum yields for single-step CT and total CT are equal; CT appears to be coherent for n = 7, 8. As detailed above, the yields of single-step CT determined from fluorescence quenching and presented in Figure 2 are lower limits on the actual yield of single-step CT. If CT to guanine competes with CT to adenine, or with conversion to other non-emissive states, then the true yield of single-step CT must be higher than the values we use for the analysis here. On the other hand, in the absence of back electron transfer, total CT is necessarily greater than or equal to the single-step component. To summarize,

$$\Phi_{em}^I - \Phi_{em}^G \leq \Phi_{CT}^G \leq \Phi_{CT,total}^G \leq \Phi_{CT,total}^{CP_G}$$

That $\Phi_{em}^I - \Phi_{em}^G$ is the same as $\Phi_{CT,total}^{CP_G}$ for n = 7, 8 implies that $\Phi_{CT}^G = \Phi_{CT,total}^G$ for these bridges, and further validates the model for the excited state dynamics that we have assumed.

Coherent CT across Domains

It is noteworthy that CT appears to be in a single step in those assemblies where the periodic variation in fluorescence quenching is a maximum. We have proposed that these periodicities in CT depend upon transient delocalized domains in the DNA duplex, and how well an assembly can structurally and dynamically accommodate such a domain. From the data presented here, it appears that when the domain is well accommodated, CT is coherent.^{5,32} Moreover, that coherence arises when the domain, including Ap, the 7–8 intervening adenines, and guanine, represents essentially a full turn of the DNA helix (Figure 3).

An important consideration, in this context, is whether delocalization itself could slow the ring-opening rate of the CPG. Both experimental and theoretical studies have clearly supported delocalized, CT-active states to be non-equilibrium and populated on the picosecond time-scale^{13–15,33}, with rapid localization of the hole onto a single nucleotide^{6d,34}. Localization of the guanine radical cation occurs on a similar time-scale as ring-opening, and certainly far faster than recombination, indicating that the hole trapping rate should be unaffected by domains.

Transition to Single Step CT

Furthermore, these data provide the first case of single-step CT overtaking incoherent CT at longer distances. This transition is opposite to that generally observed in molecular bridges.^{35–38} The changing contributions of the two mechanisms could not have been determined by solely measuring the total CT yield as a function of distance. The distance dependence for n > 4 is fit comparably by a geometric or an exponential decay (Figure S2); generally, fits of CT rates to these two decays tend to be equivalent for moderate bridge lengths.³⁹ In

fact, the distance dependence of the total yield is similar to that observed for total CT between stilbenes in photoexcited stilbene-capped DNA hairpins, despite that system being incompetent for coherent CT over more than two base pairs.⁴⁰ The geometric dependence gives an η of 2.6, corresponding to a small bias towards migration away from the ^{CPG},⁴¹ probably due to coulombic attraction to the aminopurine anion radical.⁴²

Oxidation of the Adenine Bridge

To measure oxidation of the bridge, we inserted ^{CPA}, an unnatural adenine analogue, into the adenine tract. The potential of the Ap excited state is barely adequate for adenine oxidation,²⁵ but we find rapid decomposition of ^{CPA} upon irradiation of Ap-containing duplexes (Figure S3).⁴³ As ^{CPA} is moved along the 5'-adenine tract, there is the same initial increase in yield due to charge recombination competing less favorably with trapping (Table S2). We would expect that ^{CPA} in the adenine tract would interfere with multi-step hopping of a hole to ^{CPG}. Accordingly, far less ^{CPG} decomposition is observed for Ap-A₂-^{CPA}-A₂-^{CPG} and Ap-A₂-^{CPA}-A₃-^{CPG} than the respective assemblies without ^{CPA}, Ap-A₅-^{CPG} and Ap-A₆-^{CPG} (Figure 4). For both bridge lengths, the quantum yield of ^{CPG} decomposition when multi-step transport is blocked is similar to the quantum yield of emission quenching by guanine. These results provide further support to our assignment of the yield of emission quenching as the yield of single-step CT to guanine.

We also see evidence for delocalization from the sensitivity of ^{CPA} decomposition to the sequence distal to the photooxidant. Significantly less ^{CPA} decomposition is observed for Ap-A₂-^{CPA}-A₂-^{CPG} than for Ap-A₂-^{CPA}-A₃-^{CPG}, where the only difference is the number of adenines between ^{CPA} and ^{CPG} (Table S2). For two, but not three intervening adenines, ^{CPG} is competent to compete with ^{CPA} for the radical. This sensitivity to a distal trap could be due to either polaron formation^{6,7,19} or transient delocalization along the adenine tract and ^{CPG} reporter. We have previously observed similar behavior for oxidation of the higher potential ^{CPG} near ^{CPG}, although in that case competition was not apparent for more than a single intervening adenine.⁸ Furthermore, Ap-A₃-^{CPA}-A-I and Ap-A₃-^{CPA}-A₄-I differ only in the length of the adenine tract, yet the quantum yield of ^{CPA} decomposition increases by 50% for the latter assembly. The longer adenine tract has more runs of AT base pairs that include the ^{CPA}, and hence can accommodate more low-potential delocalized orbitals. Again, both a self-trapped polaron following injection and transient delocalization prior to injection are consistent with this interpretation.

Intriguingly, ^{CPA} decomposition is insensitive to whether the distant base is inosine or guanine. When there is no guanine at the end of the adenine tract, the single-step CT pathway that leads to fluorescence quenching is eliminated. If single- and multi-step CT are in competition, eliminating single-step CT to guanine should lead to an increase in the yield of ^{CPA} oxidation, but such an increase is not observed. Hence, single- and multi-step CT must be proceeding from different populations. This is consistent with the temperature dependence of the emissive Ap picosecond decay components, which supports the presence of two different populations of assemblies; those in an initially CT-active state proceed to rapid CT, while CT for those in a less active configuration is conformationally gated.¹⁴

CONCLUSIONS

Over a long adenine tract that can accommodate well-stacked, delocalized domains, long-distance, single-step CT dominates the overall transport from aminopurine to guanine. At other separations, multi-step CT is dominant, even in sequences with shorter donor-acceptor separation, where dynamic delocalized domains do not span the construct. These results reflect the exquisite sensitivity to base stacking that has been documented and underscore the importance of sequence-dependent conformational dynamics in the mechanism and

yields of DNA-mediated CT. CT through DNA can occur effectively through transiently delocalized regions of the duplex, indeed through a fully delocalized helical turn of DNA. Significantly, models of charge migration in DNA must consider the contribution of coherent transfer over long distances.

Supplementary Material

Refer to Web version on PubMed Central for supplementary material.

Acknowledgments

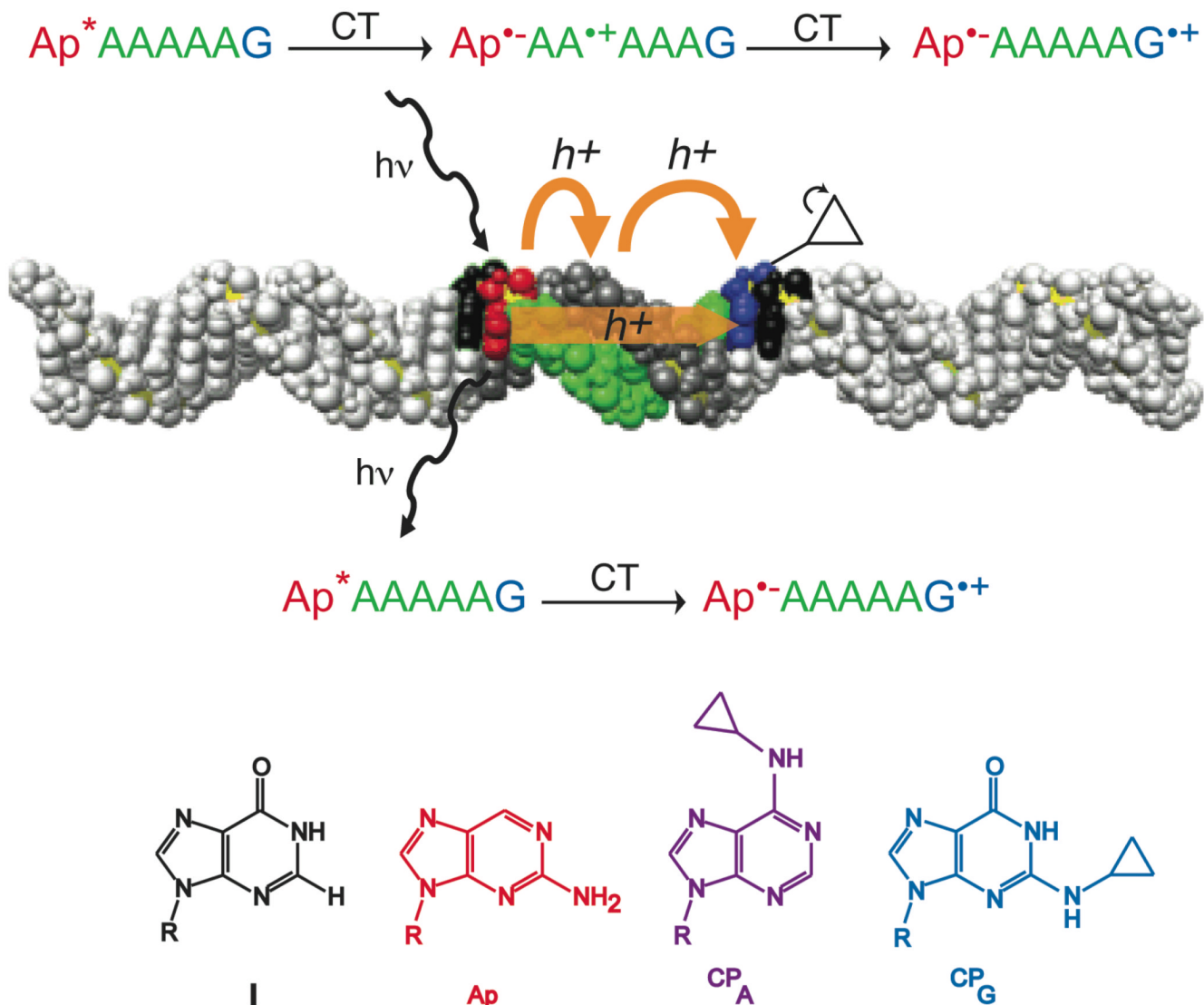
We are grateful to the National Institutes of Health (GM49216) for their support. We also thank the Caltech SURF program for a summer undergraduate fellowship (S.M.W).

References

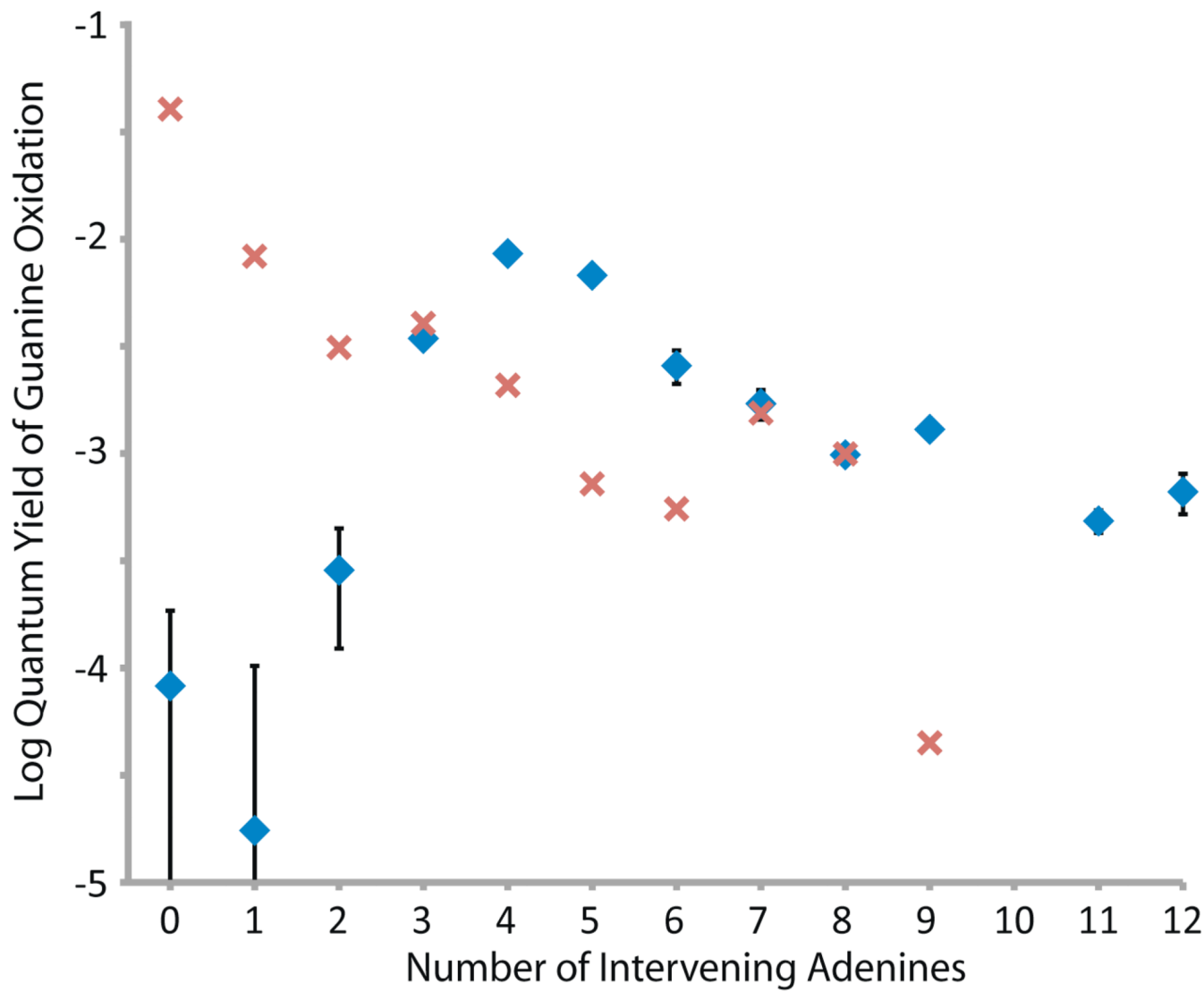
1. (a) Gorodetsky AA, Buzzo MC, Barton JK. *Bioconjugate Chem.* 2008; 19:2285–2296. (b) Genereux JC, Boal AK, Barton JK. *J. Am. Chem. Soc.* 2010; 132:891–905. [PubMed: 20047321] (c) Guo X, Gorodetsky AA, Hone J, Barton JK, Nuckolls C. *Nature Nano.* 2008; 3:163–167.
2. (a) Genereux JC, Barton JK. *Chem. Rev.* 2009; 110:1642–1662. [PubMed: 20214403] (b) Mallajosyula SS, Pati SK. *J. Phys. Chem. Lett.* 2010; 1:1881–1894. (c) Wagenknecht, H-A. *Charge Transfer in DNA: From Mechanism to Application.* Weinheim, Germany: Wiley VCH; 2005. (d) Wagenknecht H-A. *Nat. Prod. Rep.* 2006; 23:973–1006. [PubMed: 17119642]
3. Kelley SO, Barton JK. *Science.* 1999; 283:375–381. [PubMed: 9888851]
4. Nunez ME, Hall DB, Barton JK. *Chemistry & Biology.* 1999; 6:85–97. [PubMed: 10021416]
5. O'Neill MA, Barton JK. *J. Am. Chem. Soc.* 2004; 126:11471–11483. [PubMed: 15366893]
6. (a) Schuster GB. *Acc. Chem. Res.* 2000; 33:253–260. [PubMed: 10775318] (b) Barnett RN, Cleveland CL, Joy A, Landman U, Schuster GB. *Science.* 2001; 294:567–571. [PubMed: 11641491] (c) Zeidan TA, Carmieli R, Kelley RF, Wilson TM, Lewis FD, Wasielewski MR. *J. Am. Chem. Soc.* 2008; 130:13945–13955. [PubMed: 18811163] (d) Kucherov VM, Kinz-Thompson CD, Conwell EM. *J. Phys. Chem. C.* 2010; 114:1663–1666.
7. (a) Basko DM, Conwell EM. *Phys. Rev. Lett.* 2002; 88:098102. [PubMed: 11864060] (b) Conwell EM, Bloch SM, McLaughlin PM, Basko DM. *J. Am. Chem. Soc.* 2007; 129:9175–9181. [PubMed: 17585762]
8. (a) Shao F, Augustyn KE, Barton JK. *J. Am. Chem. Soc.* 2005; 127:17445–17452. [PubMed: 16332096] (b) Shao F, O'Neill MA, Barton JK. *Proc. Natl. Acad. Sci. USA.* 2004; 101:17914–17919. [PubMed: 15604138]
9. (a) Adhikary A, Kumar A, Khanduri D, Sevilla MD. *J. Am. Chem. Soc.* 2008; 130:10282–10292. [PubMed: 18611019] (b) Kobayashi K. *J. Phys. Chem. B.* 2010; 114:5600–5604. [PubMed: 20369809]
10. (a) Renger T, Marcus RA. *J. Phys. Chem. A.* 2004; 107:8404–8419. (b) Jakobsson M, Stafström S. *J. Chem. Phys.* 2008; 129:125102. [PubMed: 19045063]
11. (a) Buchvarov I, Wang Q, Raytchev M, Trifonov A, Fiebig T. *Proc. Natl. Acad. Sci. U.S.A.* 2007; 104:4794–4797. [PubMed: 17360401] (b) Conwell EM. *J. Phys. Chem. B.* 2008; 112:2268–2272. [PubMed: 18232682]
12. (a) Lewis JP, Cheatham TE III, Starikov EB, Wang H, Sankey OF. *J. Phys. Chem. B.* 2003; 107:2581–2587. (b) Hatcher E, Balaeff A, Keinan S, Venkatramani R, Beratan DN. *J. Am. Chem. Soc.* 2008; 130:11752–11761. [PubMed: 18693722] (c) Bongiorno A. *J. Phys. Chem. B.* 2008; 112:13945–13950. [PubMed: 18844392] (d) Kubar T, Kleinekathofer U, Elstner M. *J. Phys. Chem. B.* 2009; 113:13107–13117. [PubMed: 19725541]
13. O'Neill MA, Barton JK. *J. Am. Chem. Soc.* 2004; 126:13234–13235. [PubMed: 15479072]
14. O'Neill MA, Becker H-C, Wan C, Barton JK, Zewail AH. *Angew. Chem. Int. Ed.* 2003; 42:5896–5900.

15. (a) Troisi A, Orlandi G. *J. Phys. Chem. B*. 2002; 106:2093–2101. (b) Reha D, Barford W, Harris S. *Phys. Chem. Chem. Phys.* 2008; 10:5436–5444. [PubMed: 18766241] (c) Steinbrecher T, Koslowski T, Case DA. *J. Phys. Chem. B*. 2008; 112:16935–16944. [PubMed: 19049302]
16. Genereux JC, Augustyn KE, Davis ML, Shao F, Barton JK. *J. Am. Chem. Soc.* 2008; 130:15150–15156. [PubMed: 18855390]
17. (a) Hall DB, Holmlin RE, Barton JK. *Nature*. 1996; 382:731–735. [PubMed: 8751447] (b) Senthilkumar K, Grozema FC, Guerra CF, Bickelhaupt FM, Lewis FD, Berlin YA, Ratner MA, Siebbeles LDA. *J. Am. Chem. Soc.* 2005; 127:14894–14903. [PubMed: 16231945] (c) Kanvah S, Joseph J, Schuster GB, Barnett RN, Cleveland CL, Landman U. *Acc. Chem. Res.* 2009; 43:280–287. [PubMed: 19938827]
18. (a) Misiaszek R, Crean C, Joffe A, Geacintov NE, Shafirovich V. *J. Biol. Chem.* 2004; 279:32106–32115. [PubMed: 15152004] (b) Stemp EDA, Arkin MR, Barton JK. *J. Am. Chem. Soc.* 1997; 119:2921–2925.
19. Liu C-S, Hernandez R, Schuster GB. *J. Am. Chem. Soc.* 2004; 126:2877–2884. [PubMed: 14995205]
20. Williams TT, Dohno C, Stemp EDA, Barton JK. *J. Am. Chem. Soc.* 2004; 126:8148–8158. [PubMed: 15225056]
21. (a) Nakatani K, Dohno C, Saito I. *J. Am. Chem. Soc.* 2001; 123:9681–9682. [PubMed: 11572693] (b) Dohno C, Ogawa A, Nakatani K, Saito I. *J. Am. Chem. Soc.* 2003; 125:10154–10155. [PubMed: 12926921]
22. Augustyn KE, Genereux JC, Barton JK. *Angew. Chem. Int. Ed.* 2007; 46:5731–5733.
23. (a) Dohno C, Stemp EDA, Barton JK. *J. Am. Chem. Soc.* 2003; 125:9586–9587. [PubMed: 12904014] (b) Reid GD, Whittaker DJ, Day MA, Turton DA, Kayser V, Kelly JM, Beddard GS. *J. Am. Chem. Soc.* 2002; 124:5518–5527. [PubMed: 11996595]
24. O'Neill MA, Dohno C, Barton JK. *J. Am. Chem. Soc.* 2004; 126:1316–1317. [PubMed: 14759170]
25. Wan C, Fiebig T, Schiemann O, Barton JK, Zewail AH. *Proc. Natl. Acad. Sci. U.S.A.* 2000; 97:14052–14055. [PubMed: 11106376]
26. Hatchard CG, Parker CA. *Proc. R. Soc. Lon. Ser. A.* 1956; 235:518.
27. O'Neill MA, Barton JK. *Proc. Natl. Acad. Sci. USA.* 2002; 99:16543–16550. [PubMed: 12486238]
28. Somsen OJG, Keukens LB, de Keijzer MN, van Hoek A, van Amerongen H. *ChemPhysChem.* 2005; 6:1622–1627. [PubMed: 16082664]
29. Manoj P, Min C-K, Aravindakumar CT, Joo T. *Chem. Phys.* 2008; 352:333–338.
30. Wan C, Xia T, Becker H-C, Zewail AH. *Chem. Phys. Lett.* 2005; 412:158–163.
31. Takada T, Kawai K, Cai X, Sugimoto A, Fujitsuka M, Majima T. *J. Am. Chem. Soc.* 2004; 126:1125–1129. [PubMed: 14746481]
32. Valis L, Wang Q, Raytchev M, Buchvarov I, Wagenknecht H-A, Fiebig T. *Proc. Natl. Acad. Sci. USA.* 2006; 103:10192–10195. [PubMed: 16801552]
33. Adhikary A, Khanduri D, Sevilla MD. *J. Am. Chem. Soc.* 2009; 131:8614–8619. [PubMed: 19469533]
34. (a) Voityuk AA. *J. Chem. Phys.* 2005; 122:204904. [PubMed: 15945774] (b) Kinz-Thompson C, Conwell E. *J. Phys. Chem. Lett.* 2010; 1:1403–1407. (c) Kurnikov IV, Tong GSM, Madrid M, Beratan DN. *J. Phys. Chem. B*. 2002; 106:7. (d) Uskov DB, Burin AL. *Phys. Rev. B*. 2008; 78:073106.
35. (a) Weiss EA, Ratner MA, Wasielewski MR. *Top. Curr. Chem.* 2005; 257:103–133. (b) Davis WB, Svec WA, Ratner MA, Wasielewski MR. *Nature*. 1998; 396:60–63.
36. (a) Choi SH, Kim BS, Frisbie CD. *Science*. 2008; 320:1482–1486. [PubMed: 18556556] (b) Choi SH, Risko C, Ruiz Delgado MC, Kim BS, BrÈdas J-L, Frisbie CD. *J. Am. Chem. Soc.* 2010; 132:4358–4368. [PubMed: 20218660] (c) Luo L, Frisbie CD. *J. Am. Chem. Soc.* 2010; 132:8854–8855. [PubMed: 20550115]
37. (a) Paul A, Watson RM, Lund P, Xing Y, Burke K, He Y, Borguet E, Achim C, Waldeck DH. *J. Phys. Chem. C*. 2008; 112:7233–7240. (b) Paul A, Watson RM, Wierzbinski E, Davis KL, Sha A, Achim C, Waldeck DM. *J. Phys. Chem. B*. 2010; 114:14140–14148. [PubMed: 19691305]

38. Giese B, Amaudrut J, Köhler A-K, Spormann M, Wessely S. *Nature*. 2001; 412:318–320. [PubMed: 11460159]
39. Goldsmith RH, DeLeon O, Wilson TM, Finkelstein-Shapiro D, Ratner MA, Wasielewski MR. *J. Phys. Chem. A*. 2008; 112:4410–4414. [PubMed: 18422290]
40. Lewis FD, Zhu H, Daublain P, Cohen B, Wasielewski MR. *Angew. Chem. Int. Ed.* 2006; 45:7982–7895.
41. Jortner J, Bixon M, Langenbacher T, Michel-Beyerle ME. *Proc. Natl. Acad. Sci. USA*. 1998; 95:12759–12765. [PubMed: 9788986]
42. Grozema FC, Tonzani S, Berlin YA, Schatz GC, Siebbeles LDA, Ratner MA. *J. Am. Chem. Soc.* 2008; 130:5157–5166. [PubMed: 18324767]
43. The potentials of A and ^{CP}A have not been experimentally compared, and neither has been measured as a DNA-incorporated species. Electrochemical studies on free nucleosides^{21b,44} suggest that the oxidation potential of ^{CP}A might be as much as 200 mV below that of A. While we are skeptical regarding the relevance of aqueous nucleotide potentials to hole potentials in DNA, it is possible that ^{CP}A is more effective than A at intercepting the hole based on a lower potential.
44. Okamoto A, Tanaka K, Saito I. *J. Am. Chem. Soc.* 2003; 125:5066–5071. [PubMed: 12708856]
45. Munteanu MG, Vlahovicek K, Parthasarathy S, Simon I, Pongor S. *Trends Biochem. Sci.* 1998; 23:341–346. [PubMed: 9787640]

**Figure 1.**

Pathways for single-step and multi-step CT. 2-aminopurine (Ap) is selectively excited and relaxes to an excited state that is competent for oxidizing guanine (blue; bottom reaction) through the adenine bridge in a coherent single-step process or oxidizing adenine(s) (green) as an intermediate step(s). A hole on adenine can then hop to the guanine, resulting in multi-step CT (top reaction). These CT processes are in competition with emission; hence emission yield is attenuated by CT. Structures of the four unnatural bases employed are also shown. The DNA image was constructed using coordinates generated with the model.it® Server.⁴⁵

**Figure 2.**

Semilog plot of CT quantum yields as a function of bridge length for the $\text{Ap}-\text{A}_n-\text{CPG}$ series (blue diamonds), as determined by ring-opening of CPG . The experiments were repeated at least nine times, the results averaged, and the error is expressed as 90% s.e.m. Error bars that are not shown are smaller than the data point. On the same plot, single-step CT yields for the analogous duplexes are shown for comparison (red x's, data from reference 5).

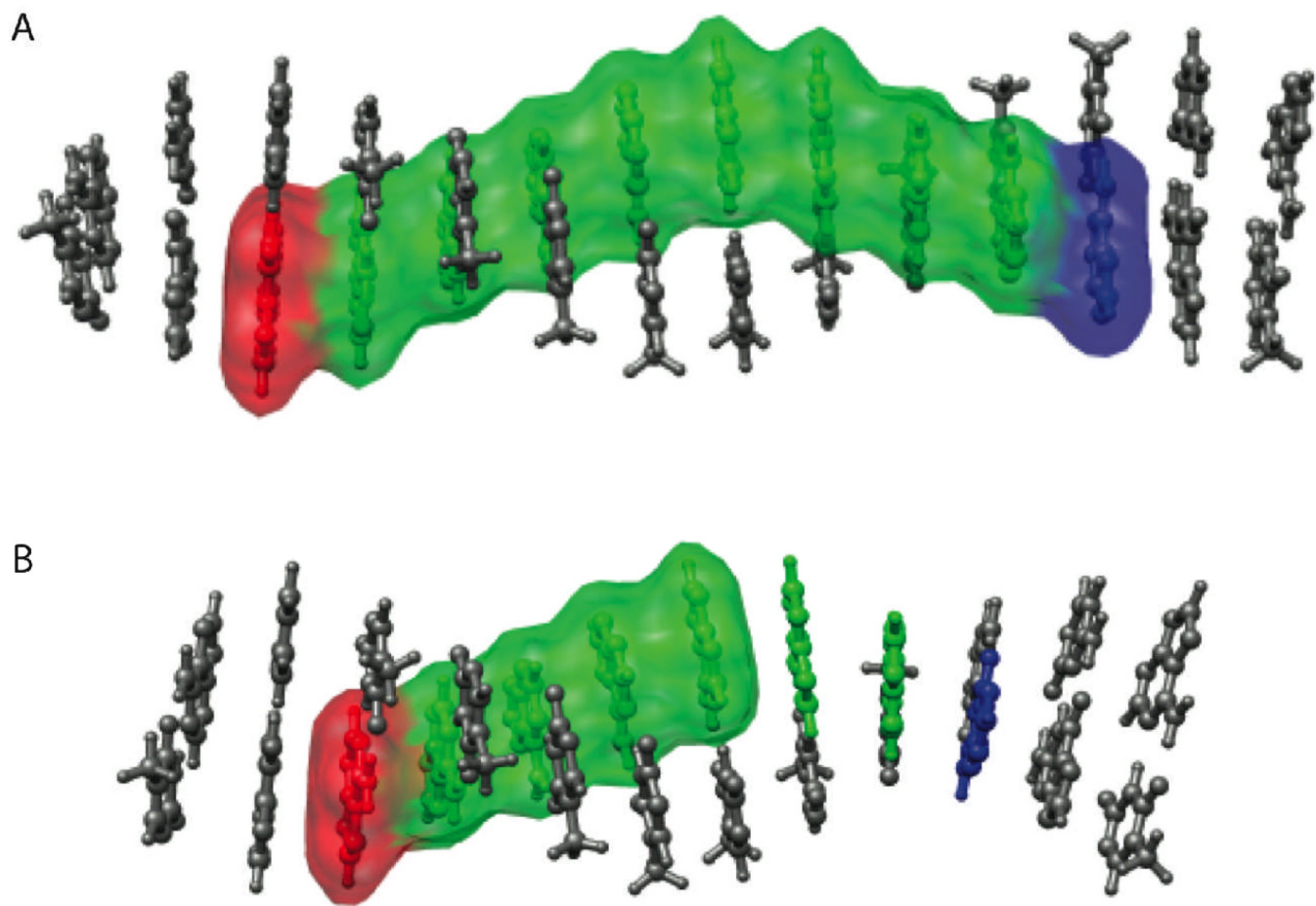
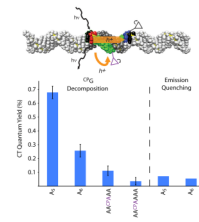


Figure 3.

The higher yield of single-step CT through the eight-adenine tract versus the six-adenine tract is a property of the sequence of the DNA, rather than the distance between the donor and the acceptor. An integer number of fully delocalized domains can be accommodated along the eight-adenine tract, allowing CT between the donor and acceptor and delocalization across the full helical turn (**A**). The six-adenine tract, below, cannot accommodate delocalized domains along its entire length (**B**), and single-step CT is limited to a less ideal bridging structure. The DNA image was constructed using coordinates generated with the model.it® Server.45

**Figure 4.**

A ^CPA inside the adenine tract disrupts multi-step CT to ^CPG by intercepting the hole. CT through the sequences Ap-A₅-^CPG and Ap-A₆-^CPG is mostly multi-step, and the intervening ^CPA disrupts CT substantially, but not totally. The remaining CT yield when multi-step transport is blocked is the same as the single-step CT yield determined for these sequences from fluorescence quenching, validating our complementary measurements of the two channels. Error bars are 90% s.e.m. The DNA image was constructed using coordinates generated with the model.it®Server.45